Pure & Appl. Chem., Vol. 57, No. 10, pp. 1391–1402, 1985.
Printed in Great Britain.

Order and disorder in transition metal carbides and nitrides: experimental and theoretical aspects

C.H. de NOVION and J.P. LANDESMAN

C.E.A.-I.R.D.I., SESI, CEN, B.P. n° 6, 92260 Fontenay-aux-Roses, France

Abstract - A general overview of the experimental data concerning long and short-range order of metalloïd vacancies in rocksalt structure transition metal carbides and nitrides is given. Hexagonal compounds M_2C and M_2N are also briefly considered. Emphasis is put on neutron scattering experiments, and new information is given, in particular on the TiC_x system. Some data concerns the vacancy-induced lattice distortions. Recent theoretical calculations of the stability of ordered phases and of pair interaction potentials, starting from the band structure of the stoichiometric compounds, are briefly presented.

INTRODUCTION

Transition metal carbides and nitrides show very remarkable properties (ref. 1) :
- high melting temperatures (≃ 4 000 °C for TaC and HfC),
- great hardness,
- metallic electrical conductivity, and even in some cases superconductivity ($T_c \simeq$ 18 K for $NbC_{0.3}N_{0.7}$),
- large departures from the stoichiometric compositions (for example $TiC_{0.50}$ to $TiC_{0.97}$),
- complex electronic structure presenting altogether metallic, covalent and ionic aspects, but dominated by the strong hybridization between the metal d and the carbon or nitrogen 2p atomic electron states (ref. 2).

Many of these carbides and nitrides can be described as a close-packed metal lattice (f.c.c. or h.c.p.), with the carbon or nitrogen atom in the center of the octahedral interstices. If these octahedral sites are not all occupied, the unoccupied sites may be considered as "vacancies" in the metalloïd sublattice. Depending on the composition and the thermal treatment, these"vacancies" may be found ordered (forming a new lattice) or disordered. "Vacancies" and metalloïd atoms form a pseudo "solid-solution", with order-disorder phenomena analogous to those encountered in metallic solid solutions $A_{1-x}B_x$.

These ordering phenomena were discovered around 1965. An experimental review was presented in 1977 (ref. 3) ; a review of phase diagram and crystallographic results obtained by Russian searchers was presented in (ref. 4). Since then, important progress was made in our knowledge and understanding of these phenomena, in particular by neutron scattering experimental studies and theoretical ab-initio calculations of phase stability and pair energy interactions from the electronic structure of the compounds.

The compounds discussed here will be :

a) The rocksalt structure monocarbides and mononitrides ; these are found for transition metals of group III (Sc, Y, La, rare-earths), IV (Ti, Zr, Hf, Th), V (V, Nb, Ta) and VI (Cr, Mo, W). Actinide monocarbides and mononitrides will not be considered here (for a review see (ref. 5)). The range of composition where these compounds are found single-phased is given in Table 1. Of course, it depends of temperature : the values of Table 1 correspond to samples obtained at room temperature after normal cooling (≃ 1 °C/s) from above 1 000 °C ; but, due to the very high migration enthalpy of the metalloïd atom (∿ 4 eV), they are more truly representative of the domain of existence around 1 000 °C. In fact, we do not know what is the stability of phases at 0 K or even at room temperature. Long annealing studies on TiC_x and TiN_x show that the low metalloïd content boundary which extends to $TiC_{0.5}$ and $TiN_{0.5}$ around 1 500 °C, restricts to $TiC_{0.60}$ and $TiN_{0.68}$ around 700 °C (refs. 4, 6, 7). The lattice parameters a_o of these compounds do not vary much with composition (typically 0.01 Å for Δx = 0.10): approximate values are given in Table 1.

For all rocksalt structure transition metal carbides, non-stoichiometry is due to carbon vacancies, the metallic sublattice remaining completely occupied, as shown by precise density

measurements (see ref. 8). At high temperature, YC_x and ThC_x can accommodate a large proportion of carbon interstitials up to chemical formulae such as MC_2. On the contrary, for some mononitrides such as TiN_x, x values larger than 1 have been observed and attributed to the presence of metal vacancies (ref. 1) ; this has not been the subject of many studies up to now, and experimental data are still somewhat conflicting.

b) The hexagonal hemicarbides and heminitrides M_2C and M_2N : these are found essentially for transition metals of columns V (V, Nb, Ta) and VI (Mo, W). In these compounds, the metal lattice is hexagonal close-packed and the metalloïd atoms occupy half of the available octahedral sites in either an ordered or disordered distribution.

ORDER-DISORDER AND LATTICE DISTORTION IN TITANIUM MONOCARBIDE

The long-range ordered structures

For $0.5 < x < 0.7$, long-range ordering of carbon vacancies occurs in TiC_x annealed below 800 °C. Goretzki first observed by powder neutron diffraction superlattice reflexions such as (1/2 1/2 1/2), (3/2 1/2 1/2), .. (ref. 9) ; he proposed a cubic superstructure of lattice parameter $b = 2\,a_o$, double from that of the NaCl primitive cell size a_o, and consistent with formula Ti_2C and space group Fd3m. It may be described as sequences of {111} carbon planes alternately 1/4 and 3/4 full. Electron diffraction observations (ref. 10) were consistent with this structure, although the small ordered domain size (∿ 300 Å) did not allow single domain diffraction.

The structure, the order-disorder transition, the kinetics of ordering and the growth of antiphase domains have been studied in detail by Moisy-Maurice et al (ref. 6) by high temperature powder neutron diffraction. The thermal dependence of the superstructure reflexion (1/2 1/2 1/2) for $TiC_{0.67}$ is shown on Fig. 1. The following order-disorder critical temperatures were determined :

. $TiC_{0.58}$: $T_c = 760 \pm 5$ °C, transition nearly of second order with critical coefficient $\beta = 0.26 \pm 0.01$, somewhat lower but not very far to the value predicted by the 3-dimensional incompressible Ising model, $\beta = 0.31$ (ref. 11) for ordering due to short-range interactions.

. $TiC_{0.63}$ (composition Ti_8C_5) : $T_c = 785 \pm 5$ °C is maximum, and shows a small first order step, confirmed by X-ray experiments (ref. 12).

. $TiC_{0.67}$: $T_c = 770 \pm 5$ °C ; more recent X-ray experiments suggest that one crosses a two-phase (ordered + disordered) region between 740 and 770 °C (ref. 12)(Fig. 1).

. $TiC_{0.71}$: $T_c \lesssim 600$ °C (determined after quench (ref. 13)).

In fact, the situation was found more complex concerning the "true" Ti_2C_{1+y} structure. Parthe and Yvon (ref. 14) pointed out that another Ti_2C structure (where the f.c.c. metalloïd sublattice consists of alternately empty and full {111} carbon planes, similarly to the Cu-Pt intermetallic alloy) of trigonal space group $R\bar{3}m$, presented powder diffraction spectra identical to that of the above Fd3m structure, if the trigonal distortion of the cubic primitive lattice is negligible. These two structures have identical atomic pair correlations up to infinity (but can be distinguished by the number of tetrahedra formed with first neighbour carbons (ref. 15), Fig. 3a) : the first and third carbon shells around a vacancy are half filled, the second shell is completely filled, and the fourth empty ; vacancies avoid to be in f.c.c. second neighbour position. Both structures can also be described as a stacking of octahedra made of carbons and vacancies and centered on a titanium (refs. 16, 17) (Fig. 9) : for the CuPt type Ti_2C, one stacks type (e) octahedra with the same orientation of all the faces containing three carbons ; for the Fd3m-Ti_2C, type (e) octahedra are stacked with the four possible <111> orientations.

Indeed, it has been shown more recently that long anneals (several days) around 730-750 °C for $TiC_{0.63}$ and $TiC_{0.67}$, lead to a trigonally distorted phase (ref. 12) (Fig. 2) : the rhombohedral angle, 90.26 °, corresponds to a slight compression along a <111> direction with negligible change of volume. This was confirmed independently by Khaenko et al (ref. 18) who found by X-ray diffraction on a single crystal $TiC_{0.60}$ new superlattice spots (110) and (001) ; the superlattice was then suggested to correspond to the formula Ti_8C_5, with the trigonal (-hexagonal) space group $R\bar{3}m$ and hexagonal lattice parameters $a_{hex} \simeq \sqrt{2}\,a_o$, $c_{hex} \simeq 2\sqrt{3}\,a_o$. This Ti_8C_5 structure may be obtained from the Fd3m-Ti_2C by filling with carbon atoms the alternate {111} planes which were 3/4 filled (Fig. 3b). But it still does not explain all the weak superstructure reflexions, such as those found near (5/8 5/8 0) on a $TiC_{0.61}$ sample annealed 7 days at 600 °C, observed by diffuse neutron scattering (ref. 19) (Fig. 4a).

Therefore, one must consider that the exact Ti_2C_{1+y} ordered structure is not fully understood : possibly, the cubic Fd3m superstructure is a metastable form evoluating toward a stable trigonal form. Both forms (for the Ti_2C composition) are degenerate in the pair potential and rigid lattice approximation : this degeneracy can only be lifted by lattice distortion, many-body ($n > 2$) atomic interactions and (perhaps) vibrational effects at $T > 0$ K. Physical property studies on ordered and disordered $TiC_{0.625}$ have shown that long-range ordering reduces the residual electrical resistivity and (slightly) the electronic specific heat (ref. 20).

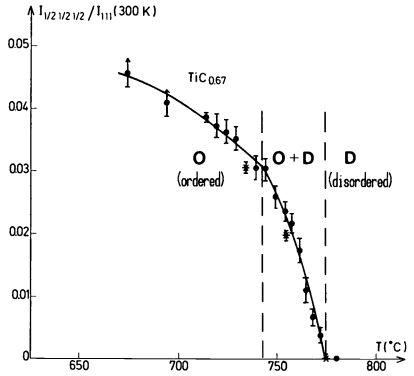

Fig. 1. Thermal dependence of the superlattice reflexion (1/2 1/2 1/2) of $TiC_{0.67}$ measured by powder neutron diffraction (refs. 6, 12).

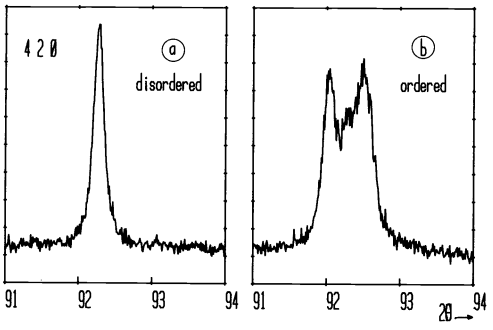

Fig. 2 : Powder X-ray diffraction spectrum of $TiC_{0.63}$ (Cu K β radiation). a : sample quenched from 1000°C, (420) f.c.c. reflexion. b : sample annealed 4 days at 750 °C : the 420 f.c.c. reflexion is splitted by the rhombohedral distortion (ref. 12).

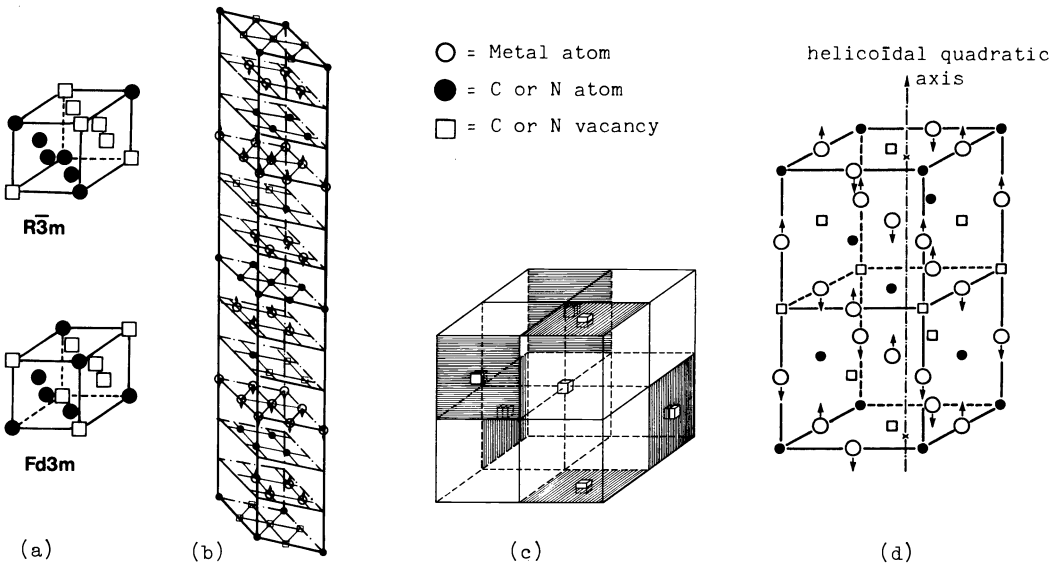

Fig. 3. Superstructures observed in cubic transition metal carbides and nitrides
a : Ti_2C, R_2C ($R\bar{3}m$-CuPt or Fd3m type) ; b : Ti_8C_5 ; c : V_8C_7 ; d : Ti_2N

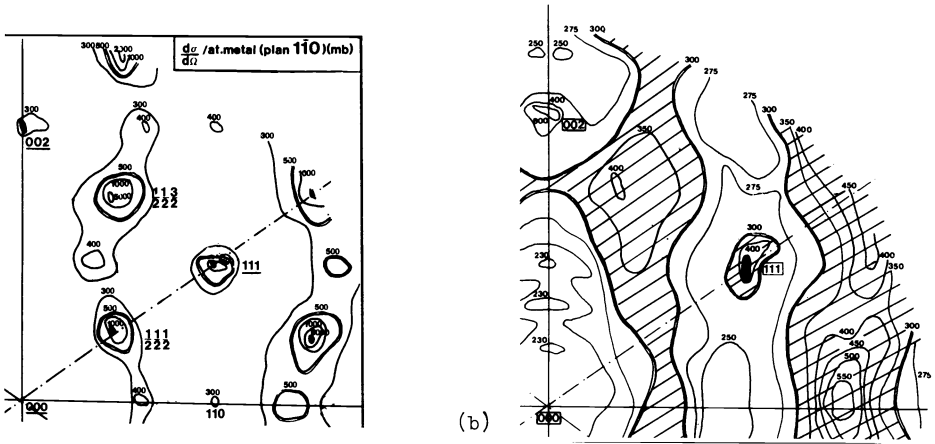

Fig. 4. Elastic diffuse neutron scattering measured at 300 K at the HFR (ILL, Grenoble, spectrometer D7, λ = 3.1 Å). $(1\bar{1}0)$ reciprocal lattice plane.
a : $TiC_{0.61}$ annealed 4 days at 600 °C ; b : $TiC_{0.79}$ (refs. 19, 23).

Short-range ordering of carbon vacancies

It was first observed on rapidly cooled $TiC_{0.5-0.7}$ samples, as diffuse streaks in the electron microdiffraction spectra (ref. 21).

Elastic neutron diffuse scattering performed at the HFR (ILL, Grenoble) at room temperature allowed to study more quantitatively this short-range ordering (refs. 19, 22, 23). For quenched $TiC_{0.64}$, broad diffuse maxima centered on (1/2 1/2 1/2), (3/2 1/2 1/2), .. (and not observed by electron diffraction) were found, superposed to the streaks ; they can be qualitatively associated to small ($\sim$ 30 Å) microdomains of Ti_2C_{1+y} (Fd3m or $R\bar{3}m$) ; recent high temperature diffuse neutron scattering experiments (ref. 24) performed up to 943 °C (largely above the critical order-disorder temperature), confirmed the existence of these maxima, which decrease with increasing temperature (Fig. 5).

For $TiC_{0.76}$ and $TiC_{0.79}$, these maxima are not observed (Fig. 4b) ; the non periodicity of the intensity in the reciprocal space is associated to static atomic relaxations ; the analysis by the Sparks and Borie first approximation (ref. 91) and least squares fit, led to the following short-range order Cowley-Warren parameters (compared to the theoretical values for Ti_2C_{1+y})(refs. 19, 22) :

	α_1	α_2	α_3	α_4	α_5
$TiC_{0.76}$	-0.003	-0.080	0.013	0.006	-0.003
$TiC_{0.79}$	+0.010	-0.175	0.010	0.025	0.015
Ti_2C_{1+y} (Fd3m or $R\bar{3}m$)	0	-1	0	+1	0

The difference between $TiC_{0.76}$ and $TiC_{0.79}$ is not easy to understand : it is probably related to different thermal treatments, and shows the necessity to perform diffuse scattering experiments at the equilibrium temperature. The short-range ordering in both samples is weak, and mostly restricted to second neighbours of the f.c.c. metalloïd sublattice. For $TiC_{0.76}$, where the above α_i are assumed to correspond to the equilibrium at 600 °C (temperature at which the sample was annealed 4 days before cooling), pair interaction potentials were calculated using the mean field approximation of Moss and Clapp (ref. 25) : $V_1 \simeq 3.2$ meV and $V_2 \simeq 7.1$ meV between first and second neighbours of the metalloïd sublattice respectively (ref. 19). The recent use of the more sophisticated "Cluster Variation Method" (ref. 26) allowed to obtain from the same experimental data : $V_1 \simeq 1.3$ meV and $V_2 \simeq 35.4$ meV (ref. 27). Although the two determinations differ quantitatively, they agree to show that the second neighbour pair interaction is positive and dominates.

Atomic relaxations

In the disordered compounds, the interatomic distances for each neighbour shell form a continuous distribution. From the elastic diffuse neutron scattering experiments mentioned above, the relative average interatomic distances C-C and C-Ti were found practically the same in $TiC_{0.76}$ and $TiC_{0.79}$ (refs. 19, 22, 23). The main effect is a reduction of the average metal-carbon first neighbour distance of 0.03 Å, compared to the lattice distance a/2. A similar result was obtained in ordered Ti_2C_{1+y} by powder neutron diffraction (ref. 6).

The fluctuations in interatomic distances due to disorder have a very strong damping effect on the EXAFS spectra (oscillations of the X-ray absorption coefficient) of the considered compound : this was studied in the case of the Ti K edge at 300 and 10 K (ref. 19). Figure 6 shows the Fourier transform of $k^3\chi(k)$ (χ = EXAFS function, k = wave-vector modulus of the photoelectron ejected from the K shell by the incident photon) for different concentrations TiC_x : the function shows peaks associated each to a shell of neighbours of a Ti situated at the origin. Increasing vacancy content results in a large damping of the EXAFS spectrum and of its Fourier transform, which in first approximation can be expressed by a static Debye-Waller factor for each shell of neighbours. A model where the six titanium surrounding a vacancy are radially shifted away by 0.07 Å, explains satisfactorily these results, in agreement with recent channeling experiments (ref. 28). The carbon static displacements are weak.

ORDERING OF METALLOID VACANCIES IN THE ROCKSALT MONOCARBIDES AND MONONITRIDES : AN EXPERIMENTAL OVERVIEW

The observed superstructures and the eventual existence of short-range ordering are listed in Table 1. For group III monocarbides, ZrC_x, ThC_x, TaC_x, one is referred to the review of (ref. 3).

Vanadium monocarbide

Two long-range ordered structures V_8C_7 and V_6C_5 are very easy to form below their (first-order type) order-disorder transition temperatures, which are respectively 1 120 and 1 260 °C (refs. 37 to 42).

TABLE 1. Composition range, lattice parameters and observed superstructures for the rocksalt structure transition metal carbides and nitrides.(S.R.O. = Short Range Ordering).

Compound	Domain of existence x = C or N/M	Lattice parameter a_0(Å) at 20°C	Ordered metalloid vacancy phases	References
ScC_x	0.3 -0.5	4.67-4.72	Sc_2C (cubic Fd3m or trigonal $R\bar{3}m$)	(ref. 29)
YC_x	0.3 -1.0*	5.06	Y_2C (trigonal $R\bar{3}m$)	(refs. 30,31)
RC_x (R = Sm → Yb)	0.4 -0.6	5.17($SmC_{0.5}$) 4.99($YbC_{0.5}$)	R_2C (trigonal $R\bar{3}m$) (R = Gd, Ho, Dy, Er)	(refs. 30,31,32)
TiC_x	0.50-0.97	4.30-4.33	Ti_2C_{1+y} (cubic Fd3m) Ti_2C_{1+y} (trigonal $R\bar{3}m$) Ti_8C_5 (trigonal $R\bar{3}m$) S.R.O.	(refs. 6,9,13) (refs. 12,14) (refs. 12,18) (refs. 21,22,23,24)
ZrC_x	0.58-0.97	4.69-4.70	Zr_2C_{1+y} (cubic Fd3m) S.R.O.	(refs. 3,9,33) (refs. 3,34)
HfC_x	0.52-0.99	4.62-4.64		
ThC_x	0.67-0.98*	5.30-5.34	S.R.O.	(refs. 34,35,36)
VC_x	0.73-0.90	4.13-4.166	V_6C_5 (trigonal $P3_1$ or $P3_2$) V_6C_5 (monoclinic B2/m) V_8C_7 (cubic $P4_132$ or $P4_332$) S.R.O.	(ref. 47) (refs. 48,49) (refs. 43,44,45) (refs. 21,54)
NbC_x	0.71-0.99	4.43-4.47	Nb_6C_5 (trigonal $R\bar{3}m$) S.R.O.	(refs. 37,57,58) (refs. 21,22)
TaC_x	0.74-0.99	4.41-4.555	Ta_6C_5 (trigonal $R\bar{3}m$)(?) S.R.O.	(refs. 37,57,63)
MoC_x+	0.69-0.75	4.27-4.28		
WC_x+	0.6 -0.7	4.22		
ScN_x	∿ 1	5.45		
YN_x	∿ 1	4.87		
RN_x (R = La → Lu)	∿ 1	5.30 (LaN) 4.80 (LuN)		
TiN_x	0.50-1.15	4.22-4.24	Ti_2N (quadratic $I4_1/amd$) S.R.O.	(refs. 7,64,65,66) (refs. 24,65)
ZrN_x	0.55-1.15	4.59-4.57		
HfN_x	0.70-1.15	4.53-4.51		
VN_x	0.73-0.99	4.07-4.14	$V_{32}N_{26}$ (quadratic $P4_2/nmc$) S.R.O.	(ref. 67)
NbN_x	0.70-1.06	4.37-4.39	Nb_4N_3 (quadratic I4/mmm)	(refs. 68,69,70)
TaN_x§	∿0.8 -0.9	4.33		
CrN_x	0.98-0.99	4.15		
MoN_x	0.4 -0.6	4.15	Mo_2N (quadratic $I4_1/amd$)	(refs. 71,72)
WN_x	∿0.5	4.13		

* Continuous solid solutions $YC_{0.5}$-$YC_{2.0}$ and Th_{metal}-$ThC_{2.0}$ at very high temperatures (> 1500°C)
\+ Phases only stable at high temperature and retained by quenching.
§ Metastable phase formed at high pressure and high temperature (T > 1900 °C) (ref. 72).

The structure of V_8C_7 (refs. 43 to 46) is cubic with lattice parameter $b = 2a_0$ (Fig. 3c), and corresponds to two enantiomorphic space groups $P4_132$ and $P4_332$ (ref. 43) ; the real crystals consist of a mixture of antiphase domains of the two groups ; vacancies are third neighbours on the carbon f.c.c. sublattice.

The crystal structure of V_6C_5 is more complicated, as two forms have been observed by electron diffraction : a trigonal form corresponding to the two enantiomorphic space groups $P3_1$ and $P3_2$ (ref. 47), and a monoclinic form of space group B2/m, which is stable at lower temperatures (T ≲ 1 000 °C) (refs. 48, 49, 50). In both forms, carbon vacancies are third neighbours on the f.c.c. metalloïd sublattice. Both structures can be described as a stacking of type (b) octahedra (Fig. 9). They consist of alternate {111} carbon planes completely and 2/3 full. They can be deduced from each other by a periodic distribution of $\{111\}_{f.c.c.}$ stacking faults. Non-stoichiometry in V_6C_5 can be accommodated by non-conservative antiphase boundaries, parallel to the $\{110\}_{f.c.c.}$ planes, and which are periodically distributed, with period up to 40 Å (refs. 49, 51).

Carbon diffusion (ref. 52) and plastic properties (ref. 37) are greatly modified by the

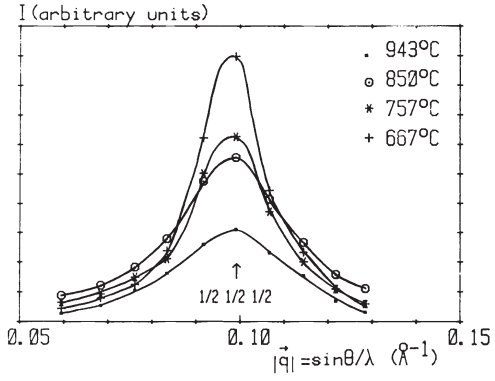

Fig. 5. Elastic neutron diffuse scattering intensity measured in the <111> reciprocal direction for $TiC_{0.64}$ at several temperatures. (ILL, Grenoble, instrument D7, λ=3.1Å)(ref.24)

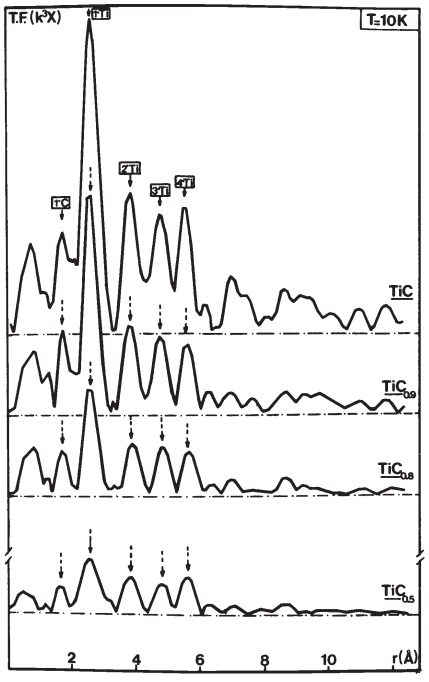

Fig. 6. Fourier transform of $k^3\chi(k)$ versus concentration in TiC_x ($\chi(k)$: EXAFS of the Ti K edge measured at 10 K) (ref. 19).

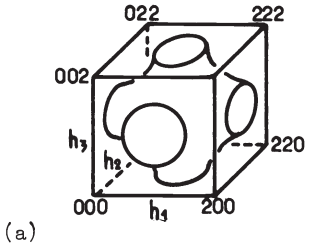

(a)

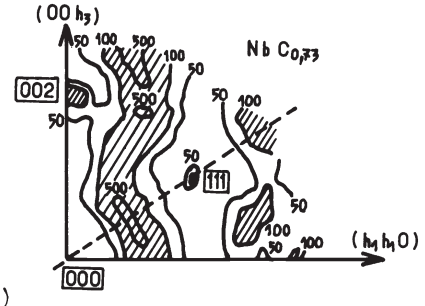

(b)

Fig. 7-a: Diffuse scattering surface found for several cubic carbides and nitrides by electron diffraction (ref. 21). b: Elastic neutron diffuse scattering measured at 300 K in the $(1\bar{1}0)$ reciprocal plane of $NbC_{0.73}$ (ref. 22)

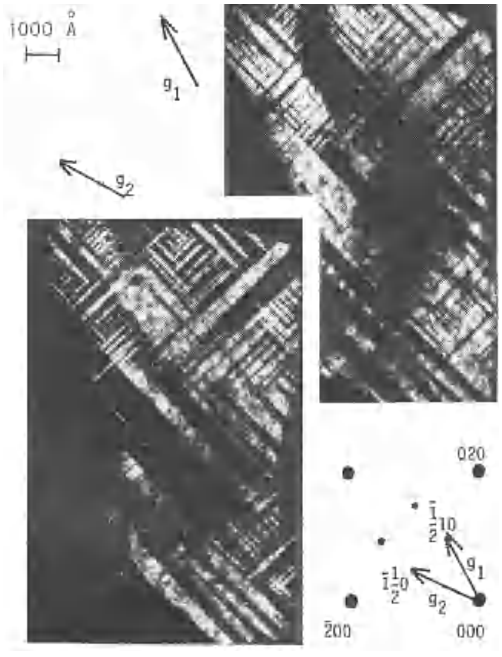

Fig. 8. Axial domain structure of ordered δ'-Ti_2N annealed 24 hours at 700°C.
The two electron micrographs correspond to dark field images, formed respectively with superstructure spots $(\bar{1}\frac{1}{2}0)$ and $(\frac{1}{2}\bar{1}0)$(ref. 7) and corresponding each to one type of axial domain.

long-range ordering of carbon vacancies in VC_x : the order-disorder transitions in V_8C_7 and V_6C_5 correspond to the brittle-to-ductile transitions. In V_6C_5 the nucleation and growth of axial domains have been studied by electron microscopy by Hannink et al (ref. 53).

The disordered structure VC_x can be retained by quench for carbon compositions lower than $VC_{0.78}$. For these, ^{51}V NMR studies (ref. 46), as well as neutron (ref. 54) and electron (ref. 21) diffuse scattering have shown the existence of short-range order between vacancies, having the same physical origin than the long-range ordered structures (i.e. vacancies preferentially third neighbours on the carbon f.c.c. sublattice). The electron microdiffraction pattern of a single crystal $VC_{0.75}$ shows, beside the f.c.c. diffraction spots, a diffuse scattered intensity distributed in first approximation on a surface of cubic symmetry, periodical in the reciprocal space (Fig. 7a). Such type of spectra have been interpreted in terms of cluster models ("transition state"), from a generalization of the Pauling rule (usually applied to ionic crystals), which suggests that the smallest blocks of the structure have as much as possible the same composition as the compound (refs. 16, 55, 56). In the case of $VC_{0.75}$, the electron diffuse scattering pattern is consistent with a mixture of randomly oriented octahedra (b) and (c) (Fig. 9), the α_2 coefficient value seeming to exclude octahedra (d) ; the model predicts the following relationship for the first short-range order coefficients : $1 + 4\,\alpha_1 + \alpha_2 = 0.222$. The α_i values deduced from the electron diffraction (where the diffuse intensity is assumed to be restricted to the surface of Fig. 7a, with a constant intensity) are : $\alpha_1 = -0.17$, $\alpha_2 = -0.30$, $\alpha_3 = +0.18$, $\alpha_4 = +0.01$, whence $1 + 4\,\alpha_1 + \alpha_2 = 0.02$ (ref. 16). A neutron diffuse scattering study (neglecting static displacements) led to : $\alpha_1 = -0.17$, $\alpha_2 = -0.20$, $\alpha_3 = +0.15$, $\alpha_4 = -0.03$ with $1 + 4\,\alpha_1 + \alpha_2 = +0.12$, in reasonable agreement with the electron diffraction data, and confirming the cluster model (ref. 54).

Niobium monocarbide

A Nb_6C_5 superstructure has been determined by electron diffraction on samples slowly cooled around 1 000 °C (refs. 37, 57) : it is isomorphous to the trigonal form of V_6C_5, as confirmed by powder neutron diffraction (ref. 58). The order-disorder transition ($T_c \simeq 1\,020$ °C) and the kinetics of ordering have been studied by high temperature neutron diffraction (ref. 58) and electrical resistivity (ref. 59).

Short-range ordering in rapidly cooled samples, similar to that found in $VC_{0.75}$, was observed by electron diffraction (ref. 21) and powder neutron diffuse scattering (ref. 60) in practically all the composition range ($NbC_{0.71-0.95}$). A single crystal elastic diffuse scattering study on $NbC_{0.73}$ shows diffuse bands (Fig. 7b) (ref. 22) corresponding to the section of the diffuse scattering surface of Fig. 7a by the $(1\bar{1}0)$ reciprocal lattice plane. The short-range order coefficients found are : $\alpha_1 = -0.095$, $\alpha_2 = -0.275$, $\alpha_3 = +0.05$, $\alpha_4 = +0.07$, whence $1 + 4\,\alpha_1 + \alpha_2 = 0.345$, allowing a similar interpretation than for $VC_{0.75}$.

Static relaxations consisting in a shift of the niobium away from their vacancies first neighbours were determined by different techniques (refs. 22, 58, 61, 62).

Titanium mononitride

Lobier and Marcon (ref. 64) found by X-ray diffraction a quadratic superstructure by annealing a $TiN_{\simeq 0.5}$ sample at 500 °C. The structure, confirmed by electron diffraction (ref. 65) and powder neutron scattering (ref. 66) is characterized by (1 1/2 0) type superlattice diffraction peaks. The quadratic cell is made of two f.c.c. primitive cells, and the space group is $I4_1/amd$ (Fig. 3d).

The ordered domain structure, consisting of antiphase domain boundaries and axial domain boundaries, was studied by electron microscopy (refs. 7, 65). Fig. 8 shows the axial domains, which form thin platelets : the deformation of the cell with ordering ($c = 2.12\,a$), and the existence of different types of axial domains with the quadratic axis taking one of the three possible $\langle 100 \rangle$ orientations, lead to strains in the sample and broadening of the diffraction peaks (ref. 7).

The order-disorder transition (first order, $\simeq$ 800 - 870 °C) and the kinetics of ordering were studied by high temperature neutron diffraction (ref. 7) ; this ordered phase ("δ' - Ti_2N") seems to be metastable as, at 750 °C, the following phase transformation sequence was directly observed (in contradiction with the phase diagram of (ref. 4)) :
quenched disordered $\delta - TiN_{0.5} \rightarrow \delta' \rightarrow \delta' + \delta + \varepsilon \rightarrow \delta - TiN_{0.68} + \varepsilon$
($\varepsilon \equiv$ quadratic antirutile structure Ti_2N_{1-y}).

Short-range ordering of nitrogen vacancies was observed at all compositions TiN_x by electron diffraction (refs. 21, 65) ; a recent neutron diffuse scattering study on $TiN_{0.80}$ (ref. 24) showed the same type of pattern as $NbC_{0.73}$ (Fig. 7b).

Other nitrides (VN_x, NbN_x, MoN_x)
A superstructure was observed in the vanadium nitride VN_x ($0.74 \lesssim x \lesssim 0.84$) by electron diffraction on samples annealed several weeks below the order-disorder transition (520 °C) (ref. 67). The structure was found tetragonal with space group $P4_2/nmc$, and $a \simeq c \simeq 2a_o$ (negligible distortion). A formula $V_{32}N_{26}$ was proposed, the nitrogen vacancies being statistically distributed between the special sites 8(g) (x = z = 1/4), 8(f), 2(b) and 4(d). Short-range ordering was observed for compositions up to $VN_{0.90}$ (ref. 67).

A tetragonal superstructure occurs in the NbN_x system for $0.70 \leqslant x \leqslant 0.85$. It could be studied by single crystal neutron diffraction : the cell is formed with two f.c.c. units (as TiN_x), with $c \simeq 2a_o$, $a \simeq a_o$, c/a = 1.98, space group $I4/mmm$, formula Nb_4N_3. Vacancies occupy the corners and the center of the tetragonal cell (structure type DO_{22}) (refs. 68, 69, 70). The order-disorder transition occurs probably at very high temperature ($T_c \simeq 1\,800$ °C) (ref. 70).

In the MoN_x system, a tetragonal superstructure Mo_2N_{1+y}, similar to Ti_2N (Fig. 3d) was observed (ref. 71). The phase diagram was studied in detail by Ettmayer and Vendl (ref. 72).

All nitride superstructures : Ti_2N, $V_{32}N_{26}$, Nb_4N_3, Mo_2N, present similar features : superlattice reflexions of the type (1 1/2 0) ; tetragonal superstructure with $c \simeq 2a_o$; body-centered tetragonal lattice of vacancies with $c \simeq 2a_o$, $a \simeq a_o$; additional vacancies are found (except for Nb_4N_3) in the z = 1/4 and z = 3/4 planes ; large distortions (except for $V_{32}N_{26}$) ; the shifts of the two first metal neighbours of a vacancy, along the z axis, differ in sign : towards the vacancy in Nb_4N_3 (by 0.04 Å), away from the vacancy in Ti_2N (by 0.12 Å).

ORDERING OF METALLOID VACANCIES IN THE ROCKSALT MONOCARBIDES AND MONONITRIDES : THEORETICAL ASPECTS

Classification of long-range ordered phases
A first classification of these phases, in terms of stacking of $\{111\}_{f.c.c.}$ planes has been proposed by Parthe and Yvon (ref. 14).

A second classification is in terms of stacking of octahedra made of carbons and vacancies, and centered on a metal atom (Fig. 9) (refs. 16, 17). The superstructures M_2C, M_2N, M_6C_5 are built with only one type of octahedra ; V_8C_7 consists in a mixture of octahedra (a) and (b), Nb_4N_3 of octahedra (b) and (d). In some short-range ordered compounds such as $VC_{0.75}$ and $NbC_{0.73}$, this model with two types of octahedra randomly oriented, succeeded to explain the shape of the diffusion scattering pattern shown Fig. 7 (ref. 16).

From the above review, very general ordering systematics are found for these compounds, and carbides and nitrides somewhat differ. In carbides, the superlattice reflexions are always of the type (1/2 1/2 1/2) and the f.c.c. second neighbour position between vacancies is forbidden ($\alpha_2 \leqslant 0$) ; in nitrides, the superlattice reflexions are of the type (1 1/2 0), and a body-centered quadratic array of vacancies ($c \simeq 2a \simeq 2a_o$) is always found. Carbides are practically undistorted by ordering ; relatively large distortions are found for some nitrides. Static displacements of metal atoms (several 0.01 Å) occur in all compounds ; in the case of the carbides, the shift is always away from the vacancy.

The most fruitfull classification of these superstructures is that based on the prediction of the Ising model, which was successfully developed for f.c.c. and b.c.c. binary alloys (refs. 15, 73, 74, 75). In this model, the carbide $MC_x\square_{1-x}$ is considered formally analogous to a substitutional f.c.c. binary alloy $A_{1-x}B_x$, the metal atom acting only on the values of the effective pair interaction energies between metalloïd atoms, V_n. Static displacements and lattice distortions are ignored. Atomic interactions are limited to pair interactions. The part of the alloy energy depending of the atomic configuration is written : $U = \sum_n p_n V_n$ (where $V_n = (V_n^{AA} + V_n^{BB} - 2V_n^{AB})/2$ is the effective pair interaction energy between n - th neighbours, which depends only of the nature of A and B and of the concentration x ; p_n is the number of A-A and B-B pairs in n-th neighbour positions. Stable ordered structures at 0 K are obtained by minimizing U.

Figure 10a shows the stable phases at 0 K for a binary alloy with first and second neighbour pair interactions V_1 and V_2 only (refs. 73, 76). The carbide phases M_2C (M = Ti, Zr, Sc, Y, T.R.) are found stable in regions I and IV ; M_6C_5 (M = V, Nb, Ta) in region I. The nitride phases (Ti_2N, Mo_2N, Nb_4N_3) are found stable in region II. Therefore this suggests that in carbides $V_2 > 0$ is the predominant pair interaction energy, and that in nitrides $V_1 > 2V_2 > 0$. No interstitial compound is found in regions III (which corresponds to many metallic alloys such as CuAu, Cu_3Au, Ni_3Fe, ..) and V (segregation). This classification confirms that carbides and nitrides form two well distinct groups. It is of course a first approximation, and longer range interactions (even if weak) are necessary to stabilize some of the ordered structures like $V_{32}N_{26}$, Ti_8C_5, V_8C_7 (ref. 77).

Calculation of the stability of long-range ordered phases at 0 K (refs. 17, 76)
This was made for the compositions M_2C and M_2N (50 % vacancies) in the Ising model with pair interactions, assuming that the energy of an ordered phase is equal to its band energy (i.e. total energy of the occupied states in the hybridized metalloïd 2p-metal d bands). The electronic density of states was calculated for the four possible ordered structures : (i) type CuPt - $R\bar{3}m$ (or Fd3m) (Fig. 3a), (ii) type Ti_2N (space group $I4_1/amd$, Fig. 3d), (iii) type CuAu (alternate Cu and Au {001} planes), (iv) segregation, which are respectively stable in regions I-IV, II, III and V of Fig. 10a. The calculations were made by the recursion method (ref. 78), starting from a tight-binding interpolation scheme for the stoichiometric compound, fitted on a self-consistent APW band structure of NbC (ref. 79). The parameters (ten transfer integrals and three atomic levels) were kept constant from NbC to M_2C (M = any transition metal).

Results are shown on Fig. 11. The CuPt type phase (or Fd3m) was found stable in a large electron concentration range ($0.22 < N_e < 0.50$, N_e = fractional occupation of the 2p-d bands containing 10 + 6 x states per molecule MC_x). This is in agreement with the observation of this phase for the carbides of groups III and IV transition metals (for V_2C, Nb_2C, Ta_2C, the metal lattice is hexagonal and the calculations cannot be compared with experiment).

But the structure observed for the nitrides (Ti_2N, Mo_2N) is not explained by this calculation ; changing the input parameters (N-N coupling, 2p level energy, crystal-field parameters) did not allow to open a significant stability zone for the Ti_2N type phase (ref. 17).

Calculation of effective pair interaction energies from the electronic structure (refs. 17,83)
In the generalized perturbation method (GPM) (refs. 80-83), the order energy of the alloy, written as a sum of interatomic pair interactions V_i, is obtained by a perturbation development from the completely disordered alloy described by the tight-binding coherent potential average medium (ref. 81). It has been shown for transition metal alloys, that the cluster interactions, concentration dependent, decrease rapidly with increasing number n of atoms in the cluster ($n \geqslant 3$) (ref. 80). In the case of transition metal carbides, the good agreement of the relative stability energies of the ordered phases calculated from the V_i obtained by the GPM, with those obtained by the recursion method, argues for the validity of the pair potential approximation (ref. 17).

GPM pair interaction energies, calculated with the same input parameters as for the recursion method, are given in Fig. 12 for the carbides of compositions M_2C and M_6C_5. One sees that the second neighbour pair interaction V_2 dominates and is positive in the electron concentration region where are observed the carbide superstructures ; this is in agreement with experiment, in particular with the pair potentials deduced from neutron diffuse scattering on $TiC_{0.76}$ (see above and (refs. 19, 27)). The dependence of V_1 and V_2 with N_e has been explained in terms of arguments of the moments of the electronic density of states (refs. 17, 84).

To explain the nitrides, one has to obtain a zone where $V_1 > 2V_2 > 0$ (the existence of V_6C_5 and Nb_6C_5 requires also a positive V_1 around $N_e = 0.44$). By (i) changing the ratio of two transfer integrals between metalloïd 2p and metal d orbitals, from the value deduced from the interpolation scheme ($pd\pi/pd\sigma = -0.3$ instead of -0.56), (ii) suppressing the direct N-N coupling, (iii) lowering the nitrogen atomic 2p level (shift of -0.1134 Rydbergs) : one obtains $V_1 > V_2 > 0$ in the region $0.47 < N_e < 0.53$.

The V_1 and V_2 values calculated for different carbides and nitrides with $pd\pi/pd\sigma = -0.3$, are reported on Fig. 10b : one sees a qualitative agreement with the predictions of the Ising model ; carbides and nitrides are well separated, but the domain of nitrides in Fig. 10b is larger than domain II of Fig. 10a.

Clearly, if the calculation from the electronic structure explains with some success the experimental behaviour, something is missing in the model : role of lattice distortions, or short-range first neighbour interactions not taken into account by the tight-binding hamiltonian used in this study (ref. 17). Further quantitative progress will need exact band structure calculations for the long-range ordered superstructures.

ORDERING OF METALLOID ATOMS IN THE HEXAGONAL CLOSE-PACKED HEMICARBIDES AND HEMINITRIDES

In these compounds, the octahedral sites of the h.c.p. metal cell form a simple hexagonal lattice, half occupied by metalloïd atoms at the stoichiometric composition M_2X. At room temperature, long-range ordering of the metalloïd atoms is always found, and the compounds M_2C and M_2N can be classified into five ordered structures labelled (a) to (e) :
(a) CdI_2 antitype (e.g. Ta_2C), (b) $CaCl_2$ antitype, (c) ε-Fe_2N type (e.g. V_2N, Nb_2N, W_2C), (d) ζ-Fe_2N type (e.g. V_2C, Mo_2C), (e) ξ-Nb_2C type.(For a review, see (refs. 1, 37, 85)). The

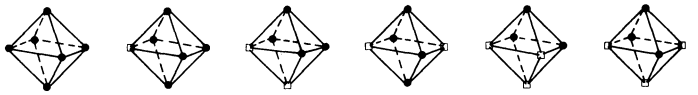

	a	b	c	d	e	f
Octahedra						
Phases	A	A_5B	A_2B	-	AB	A_2B_2
Space groups	fcc Fm3m	$P3_1$ or B2/m	B2/m		Fd3m or $R\bar{3}m$	$I4_1/amd$
Carbides, nitrides	MC, MN	V_6C_5, Nb_6C_5	-	-	Ti_2C, R_2C,..	Ti_2N, Mo_2N

Fig. 9. Phases obtained by stacking octahedra of a single type.

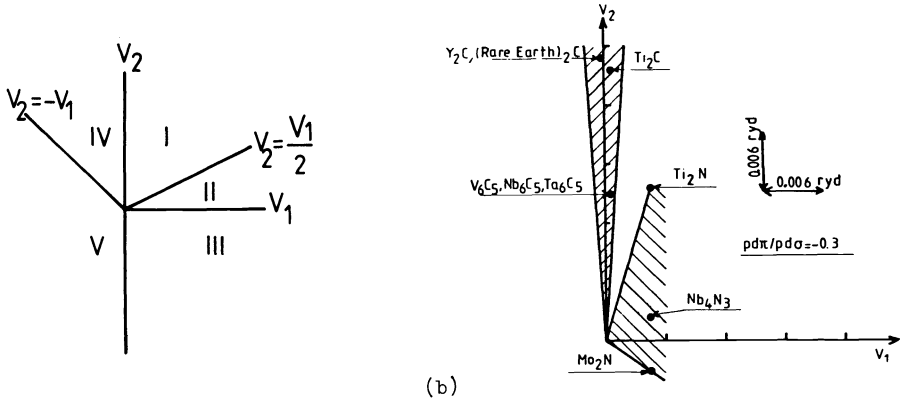

Fig. 10. a) Fundamental states of the Ising model with pair interactions V_1 and V_2 for an f.c.c. substitutional alloy $A_{1-x}B_x$ (at 0 K). Stable phases are given in the text. b) Pair potentials V_1 and V_2 calculated for different ordered carbides and nitrides by the generalized perturbation method (ref. 17).

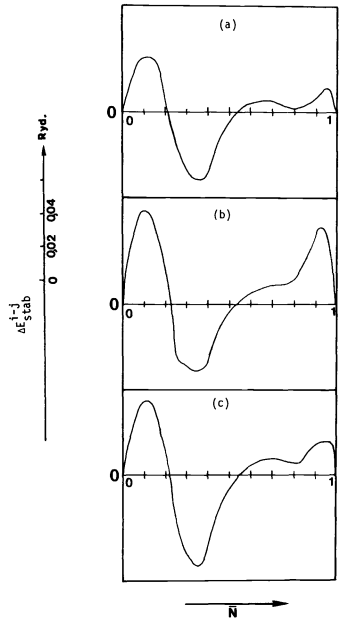

Fig. 11. Relative stability energies calculated by the recursion method (ref. 17) for cubic carbides M_2C.
a : CuPt-Ti_2N ; b : CuPt-segregation ;
c : CuPt-CuAu.

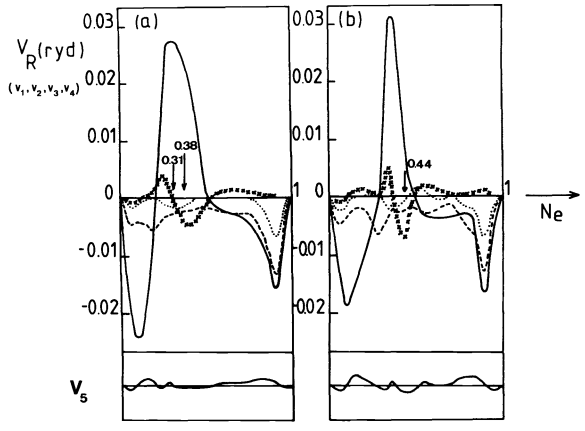

Fig. 12. Pair potentials calculated for cubic carbides by the generalized perturbation method, versus the electronic concentration.
a : M_2C ; b : M_6C_5;xxxx : V_1 ; —— : V_2
.... : V_3 ; ---- : V_4
N_e = 0.31 for R_2C, 0.38 for Ti_2C,
0.44 for V_6C_5 (ref. 17).

ordered phases have all the following common property that carbon atoms and vacancies occupy alternate octahedral sites on interstitial rows parallel to the c axis. It is generally assumed that at very high temperatures, disordering of carbons and vacancies occurs, resulting in the L'_3 type hexagonal structure. Recent high temperature diffraction studies, performed at the HFR (ILL, Grenoble), have shown the following phase transitions (ref. 85) :
. for W_2C : type (c) structure - 1 800 °C → L'_3 structure
. for Mo_2C : type (d) structure - 1 400 °C → type (c) structure - 2 000 °C → L'_3 structure

The compounds V_2C, Nb_2C and Ta_2C, and their binary pseudo-solid solutions $(V_{1-x}Nb_x)_2C$, .., have been studied by electron diffraction by Hiraga and Hirabayashi (refs. 86, 87, 88). For quenched samples, one observes diffuse scattering concentrated only in the reciprocal lattice planes 00.ℓ (ℓ = 2n + 1) normal to the c* axis, suggesting that the alternate carbon-vacancy (C - □) rows in the c direction remain at high temperature, and that disordering occurs only between the rows. The system can be analysed in terms of pair interactions between the two states α and β of interstitial C - □ rows (α ≡ C - □ - C - □ - ..), (β ≡ □ - C - □ - C - ..) and is formally identical to the Ising triangular lattice array theoretically studied in (refs. 89, 90).

REFERENCES

1. L.E. Toth, Transition Metal Carbides and Nitrides, Academic Press, New York (1971).
2. A. Neckel, Int. J. Quantum Chem. 23, 1317-1353 (1983).
3. C.H. de Novion and V. Maurice, J. Physique Colloq. 38, C7, 211-220 (1977)
4. B.V. Khaenko, Neorg. Mater. 15, 1535-1543 (1979)
5. D.J. Lam, J.B. Darby Jr. and M.V. Nevitt, The Actinides : Electronic Structure and Related Properties, Vol. II, p. 119, Academic Press, New York (1974).
6. V. Moisy-Maurice, N. Lorenzelli, C.H. de Novion and P. Convert, Acta Met. 30, 1769-1779 (1982).
7. A. Alamo and C.H. de Novion, Seventh Int. Conf. on Transition Element Compounds, Grenoble 21-25 june 1982, paper II.A.1, and to be published.
8. E.K. Storms, The Refractory Carbides, Academic Press, New York (1967).
9. H. Goretzki, Phys. Stat. Sol. 20, K 141-143 (1967).
10. P.S. Bell and M.H. Lewis, Phil. Mag. 24, 1247-1251 (1971).
11. C. Domb, Phase Transitions and Critical Phenomena, vol. 3, Academic Press, New York (1974).
12. N. Lorenzelli, to be published.
13. V.T. Em, I. Karimov, V.F. Petrunin, I. Khidirov, I.S. Latergaus, A.G. Merzhanov, I.P. Borovinskaya and V.K. Protudina, Sov. Phys. Crystallogr. 20, 198-199 (1975)
14. E. Parthe and K. Yvon, Acta Cryst. B 26, 153-163 (1970).
15. M.J. Richards and J.W. Cahn, Acta Met. 19, 1263-1277 (1971).
16. M. Sauvage and E. Parthe, Acta Cryst. A 28, 607-616 (1972) and A 30, 239-246 (1974).
17. J.P. Landesman, Thesis, Université de Strasbourg (January 1985).
18. B.V. Khaenko, S.Y. Galab and M.P. Arbuzov, Soviet. Phys. Crystallogr. 25, 63-67 (1980).
19. V. Moisy-Maurice, Report CEA-R-5127 (1981).
20. N. Lorenzelli, R. Caudron, J.P. Landesman and C.H. de Novion, to be published.
21. J. Billingham, P.S. Bell and M.H. Lewis, Acta Cryst. A 28, 602-606 (1972)
22. V. Moisy-Maurice, C.H. de Novion, A.N. Christensen and W. Just, Solid State Commun. 39, 661-665 (1981)
23. V. Moisy-Maurice, C.H. de Novion, N. Lorenzelli and A.N. Christensen, Science of Hard Materials, p. 83, Plenum Press, New York (1983).
24. J.P. Landesman, C.H. de Novion, N. Lorenzelli, A.N. Christensen, M. Schärpf and W. Just, Report of ILL experiments n° 7-03-241 and 7-03-258, Institut Laue-Langevin, Grenoble (1985) and to be published.
25. P.C. Clapp and S.C. Moss, Phys. Rev. 142, 418-427 (1966) and 171, 754-763 (1968). S.C. Moss and P.C. Clapp, Phys. Rev. 171, 764-777 (1968).
26. R. Kikuchi, Phys. Rev. 81, 988-1003 (1951) and J. Phys. Colloq. 38, C7, 307-313 (1977).
27. D. Gratias and P. Cenedese, unpublished.
28. R. Kaufmann and O. Meyer, Solid State Commun. 51, 539-543 (1984).
29. H. Rassaerts, H. Nowotny, G. Vinek and F. Benesovsky, Monatsh. für Chemie 98, 460-468 (1967).
30. G. Déan, R. Lallement, R. Lorenzelli and R. Pascard, Comptes-rendus Hebd. Sean. Acad. Sci. 259, 2442-2444 (1964).
31. R. Lallement, Report CEA-R-3043 (1966).
32. G.L. Bacchela, P. Meriel, M. Pinot and R. Lallement, Bull. Soc. Franç. Miner. Crist. 89, 226-228 (1966).
33. I. Karimov, V.T. Em, I.S. Latergaus, T.M. Myasishcheva, D. Ya. Khvatinskaya, I.P. Borovinskaya and V.T. Protudina, Fiz. Met. Metalloved. 41, 1094-1096 (1976).
34. C.H. de Novion, Actinides in Perspective, p. 175, Pergamon Press, Oxford (1982).
35. C.H. de Novion, B.E.F. Fender and W. Just, Plutonium 1975 and other Actinides, p. 893 North-Holland/Elsevier, Amsterdam (1976).

36. V. Moisy-Maurice, C.H. de Novion and P. Convert, Acta Cryst. A 36, 916-921 (1980).
37. M.H. Lewis, J. Billingham and P.S. Bell, Electron Microscopy and Structure of Materials p. 1084, Univ. of California Press, Berkeley (1972).
38. T. Lola-Athanassiadis, Note CEA-N-2109 (1980).
39. L.W. Shacklette and W.S. Williams, J. Appl. Phys. 42, 4698-4703 (1971).
40. G. Emmons, Ph. D. Thesis, Univ. of Illinois at Urbana-Champaign (1972).
41. W.S. Williams, High Temp. High Press. 4, 627-638 (1972).
42. A. Bathellier, Thesis, Université d'Orsay (1984).
43. C.H. de Novion, R. Lorenzelli and P. Costa, Comptes-Rendus Hebd. Séan. Acad. Sci. 263, 775-778 (1966).
44. Y. Guérin and C.H. de Novion, Rev. Int. Hautes Temp. et Refract. 8, 311-314 (1971).
45. A.W. Henfrey and B.E.F. Fender, Acta Cryst. B 26, 1882-1883 (1970).
46. C. Froidevaux and D. Rossier, J. Phys. Chem. Solids 28, 1197-1209 (1967).
47. J.D. Venables, D. Kahn and R.G. Lye, Phil. Mag. 18, 177-192 (1968).
48. J. Billingham, P.S. Bell and M.H. Lewis, Phil. Mag. 25, 661-672 (1972).
49. H. Hiraga, Phil. Mag. 27, 1301-1312 (1973).
50. M.P. Arbuzov, B.V. Khaenko, V.G. Fak and Yu.F. Nosachev, Ukr. Fiz. Zh. 22, 291 (1977).
51. M.H. Lewis and J. Billingham, Phil. Mag. 29, 241-252 (1974).
52. S. Sarian, J. Phys. Chem. Solids 33, 1637-1643 (1972).
53. R.H.J. Hannink, M.J. Murray and M.E. Packer, Phil. Mag. 24, 1179-1195 (1971).
54. M. Sauvage, E. Parthé and W.B. Yelon, Acta Cryst. A 30, 597-599 (1974).
55. M. Brunel, F. de Bergevin and M. Gondrand, J. Phys. Chem. Solids 33, 1927-1941 (1972).
56. R. de Ridder, G. Van Tendeloo, D. Van Dyck and S. Amelinckx, Phys. Stat. Solidi (a) 38 663-674 (1976).
57. J.D. Venables, M.H. Meyerhoff, Sol. State Chem., N.B.S. Special Publ. 364, 583-590 (1972)
58. J.P. Landesman, A.N. Christensen, C.H. de Novion, N. Lorenzelli and P. Convert, J. Phys. C : Solid State Phys. 18, 809-823 (1985).
59. L.C. Dy and W.S. Williams, J. Appl. Phys. 53, 8915-8927 (1982).
60. B.E.F. Fender, Chemical Applications of Thermal Neutron Scattering p. 261, Oxford University Press, Oxford (1973).
61. T.H. Metzger, J. Peisl and R. Kaufmann, J. Phys. F : Metal Phys. 13, 1103-1113 (1983).
62. R. Kaufmann and O. Meyer, Phys. Rev. B 28, 6216-6226 (1983).
63. D.J. Rowcliffe and G. Thomas, Mat. Sc. and Eng. 18, 231-238 (1975).
64. G. Lobier and J.P. Marcon, Comptes-Rendus Hebd. Sean. Acad. Sci. 268, 1132-1135 (1969).
65. S. Nagakura and T. Kusunoki, J. Appl. Cryst. 10, 52-56 (1977).
66. J.P. Landesman, A.N. Christensen and A. Alamo, to appear in Acta Cryst. C (1985).
67. T. Onozuka, J. Appl. Cryst. 11, 132-136 (1978).
68. N. Terao, Jap. J. Appl. Phys. 4, 353-367 (1965).
69. G. Heger and O. Baumgartner, J. Phys. C : Solid State Phys. 13, 5833-5841 (1980).
70. A.N. Christensen, R.G. Hazell and M.S. Lehmann, Acta Chem. Scand. A 35, 111-115 (1981).
71. D.A. Evans and K.H. Jack, Acta Cryst. 10, 833-834 (1957).
72. P. Ettmayer and A. Vendl, Science of Hard Materials p. 47, Plenum Press, New York (1983).
73. S.M. Allen and J.W. Cahn, Acta Met. 20, 423-433 (1972).
74. J. Kanamori and Y. Kakehashi, J. Physique Colloq. 38, C7, 274-279 (1977).
75. A. Finel and F. Ducastelle, Mat. Res. Soc.Symp. Proc. 21 p. 293, North-Holland/Elsevier, Amsterdam (1984).
76. J.P. Landesman, P. Turchi, F. Ducastelle and G. Treglia, Mat. Res. Soc. Symp. Proc. 21, p. 363, North-Holland/Elsevier, Amsterdam (1984).
77. J. Kanamori, Modulated Structures, AIP Conf. Proc. n° 53, p. 117, American Institute of Physics, New York (1979).
78. R. Haydock, Solid State Phys. 35, p. 216, Academic Press, New York (1980).
79. K. Schwarz, J. Phys. C : Solid State Phys. 10, 195-210 (1977).
80. A. Bieber, F. Gautier, G. Treglia and F. Ducastelle, Solid State Commun. 39, 149-153 (1981).
81. B. Velicky, S. Kirkpatrick and H. Ehrenreich, Phys. Rev. 175, 747-766 (1968).
82. F. Ducastelle and F. Gautier, J. Phys. F : Metal Phys. 6, 2039-2062 (1976).
83. J.P. Landesman, G. Treglia, P. Turchi and F. Ducastelle, this conference and to appear in J. de Physique (1985).
84. F. Ducastelle, Mat. Res. Soc. Symp. Proc. 21, p. 375, North-Holland/Elsevier, Amsterdam (1984).
85. J. Dubois, T. Epicier, C. Esnouf, G. Fantozzi and P. Convert, Report of ILL experiment n° 5-21-175, Institut Laue-Langevin (Grenoble, 1984) and to be published.
86. K. Hiraga and M. Hirabayashi, J. Physique Colloq. 38, C 7, 224-226 (1977).
87. K. Hiraga and M. Hirabayashi, Modulated Structures, AIP Conf. Proc. n° 53, p. 276, American Institute of Physics, New York (1979).
88. K. Hiraga and M. Hirabayashi, J. Appl. Cryst. 13, 17-23 (1980).
89. Y. Tamaka and N. Uryu, Prog. Theor. Phys. 55, 1356-1372 (1976).
90. M. Kaburagi and J. Kanamori, J. Phys. Soc. Japan, 44, 718-727 (1978).
91. C.J. Sparks and B. Borie, Local Atomic Arrangements Studied by X-Ray Diffraction, p. 5, Gordon and Breach, New York (1966).